Search for the Ideal Plasmonic Nanoshell: The Effects of Surface Scattering and Alternatives to Gold and Silver

ARTICLE *in* THE JOURNAL OF PHYSICAL CHEMISTRY C · FEBRUARY 2009

Impact Factor: 4.77 · DOI: 10.1021/jp810808h

3 AUTHORS:

Martin G Blaber
Seagate Technology
36 PUBLICATIONS **911** CITATIONS
SEE PROFILE

Matthew David Arnold
University of Technology Sydney
54 PUBLICATIONS **792** CITATIONS
SEE PROFILE

Michael J Ford
University of Technology Sydney
117 PUBLICATIONS **1,730** CITATIONS
SEE PROFILE

THE JOURNAL OF PHYSICAL CHEMISTRY C LETTERS

2009, *113,* 3041–3045
Published on Web 01/30/2009

Search for the Ideal Plasmonic Nanoshell: The Effects of Surface Scattering and Alternatives to Gold and Silver

Martin G. Blaber, Matthew D. Arnold, and Michael J. Ford*

Department of Physics and Advanced Materials and Institute for Nanoscale Technology, University of Technology, Sydney, 15 Broadway, Sydney 2007, New South Wales, Australia

Received: December 9, 2008; Revised Manuscript Received: January 16, 2009

The optical absorption efficiency of nanospheres and nanoshells of the elements Na, K, Al, Ag, and Au are compared, and the effects of surface scattering, as introduced by the billiard model [Moroz, A. *J. Phys. Chem. C* **2008**, *112* (29), 10641−10652] are discussed. We find that the introduction of surface scattering has comparatively little effect on the optimized absorption efficiency of nanospheres, with the maximum absorption efficiency of K nanospheres falling from 14.7 to 13.3. Conversely, the reduction in absorption efficiency in nanoshells is substantial. This effect is compounded in metals with higher plasma frequency. We show that the high comparative plasma frequencies in silver and gold result in a greatly reduced optimized absorption efficiency when compared to nanoshells in the absence of surface scattering. Whereas sodium and potassium, with low plasma frequencies, are not affected as much.

Plasmonics has applications in a variety of fields including super resolution planar lens lithography,[1−3] medical therapeutics and diagnostics technologies,[4−7] subwavelength color imaging systems,[8] high throughput communications and processing systems,[9] portable extreme UV lasers,[10] and solar glazing for energy efficient windows.[11] Most of these technologies rely on the strength and position of the surface plasmon on nanorods, nanoshells, or nanotriangles and the fact that the nanoparticle will absorb incident light well at the resonance wavelength. The optical properties of nanorods and nanoshells have previously been discussed[12] and compared.[13−15] In both cases the plasmon resonance can be tuned across a wide wavelength range by changing the aspect ratio. The aspect ratio is defined as length on width for nanorods and inner radius on outer radius, (r_i/r_o), for nanoshells. Gold nanorods give a larger absorption per unit volume; however, nanoshells have the distinct advantage that their optical properties are both orientation and polarization independent. Also, although the most efficient way of making nanorods[16] and nanoshells[17] is via wet chemistry, nanoshells or nanocaps can be made by evaporation or sputtering of the metal onto polystyrene spheres.[18,19] Production of nanorods in this fashion requires a more complex electrochemical templating technique.[20] A similar alumina templating technique applicable to reactive metals produces short, defective tubes rather than rods.[21] Considerable progress has been made in the application of gold nanoshells in thermal therapeutic treatment of cancer.[22]

Previously, we have investigated the merit of different metal nanospheres for use in plasmonics.[23] An analysis of 26 different, alkali, noble, and transition metals showed that although gold and silver are the most commonly used metals for plasmonics they are by far suboptimal. The question addressed here is how this extends to metal nanoshells, particularly if the influence of surface scattering is taken into account. A rule of thumb is often used in connection with surface scattering from solid gold spheres where the effect becomes appreciable for spheres below about 5 nm in radius, and experimental data support this assertion.[24] For shells, however, the optimum geometry may involve a very thin shell where surface scattering can become important.

Many metals have limited applicability as plasmonic materials due to their chemical reactivity. The alkali metals are prime examples. The absorption efficiencies of alkali metal nanospheres are substantially higher than those of the noble metals, but they have had limited practical application, at least to date, due to their extreme reactivity. However, applications such as optical nanocircuits, solar glazings, and UV lasers where direct contact with water or other oxidizing agents does not occur may provide situations where a passivating layer can be used.

The spectral selectivity of gold and silver nanoshells has been discussed by Schelm and Smith.[25] They note that long wavelength resonances require thin shells, which in turn require a large outer radius to ensure low surface scattering and ease of manufacture, and this in turn results in a large scattering efficiency.

Schelm and Smith have discussed the optimization problem for shells, in the context of maximizing infrared selectivity for window glazing applications. In the present work, we have set out to optimize the absorption efficiency of nanoshells irrespective of the resonant wavelength, and in all cases considered, our optimum particles are small and scattering plays an insubstantial role.

In this paper we investigate, using Mie theory, the optical absorption of nanoshells composed of various metallic elements in order to identify the optimum geometry and material taking into account surface scattering using the simple billiard scattering model of Moroz.[26]

* To whom correspondence should be addressed. E-mail: mike.ford@uts.edu.au.

10.1021/jp810808h CCC: $40.75

TABLE 1: Optical Data Used for the Addition of Billiard Scattering to the Bulk Experimental Permittivity

element	ω_p (eV)	γ_{intra} (eV)	V_F (10^6 m/s)[30]
Ag	9.6[31]	0.0228[32]	1.39
Au	8.55[31]	0.0184[32]	1.40
Al	15.3[33]	0.5984[34]	2.03
Na	5.71[33]	0.0276[35]	1.07
K	3.72[33]	0.0184[35]	0.86

We use the program BHCOAT,[27] a numerical solution to Mie theory for multiply coated spheres to calculate the absorption efficiency, Q_{abs}, of nanospheres and nanoshells. Bulk dielectric constants were taken from Weaver and Frederikse.[28] The spheres and shells were embedded in vacuum and shell cores were also vacuum. Shell geometries were sampled with a Gaussian distribution designed to include a large number of steps in the vicinity of the solid sphere limit (aspect ratio 0) and the infinitely thin shell limit (aspect ratio 1), with comparatively few points in between. We have included the full multipole expansion of Mie theory to ensure that symmetric and antisymmetric multipole modes contribute to the spectra.

For structures with high aspect ratios, that is shells with a thickness of a few nanometers or spheres with diameters of a few nanometers, the mean free path of the electrons is comparable to this critical size. Surface scattering can then reduce the absorption efficiency and broaden the plasmon resonance. We have included this effect in our model using the recently derived billiard scattering model by Moroz[26] to modify the bulk dielectric. This model provides a method for calculating the damping term associated with surface scattering but requires invoking an analytical model for the dielectric function in order to modify the experimental bulk dielectric. We follow the commonly used method of permittivity augmentation by Kreibig[29] where a Drude model is used to incorporate this additional damping but is applied in such a way that interband transitions are not neglected.

The intraband contribution to the permittivity can be described by the Drude model

$$\varepsilon_D(\omega) = 1 - \frac{{\omega_p}^2}{\omega(\omega + i\gamma)} \quad (1)$$

where ω_p is the bulk plasma frequency and γ is the intraband damping term (inverse of the relaxation time τ). Using the experimentally determined values for ω_p and $\gamma = \gamma_{intra}$ given in Table 1, we can calculate this intraband component, and by adding the mean free path dependent damping, $\gamma = \gamma_{intra} + \gamma(L_B)$, from the billiard model, correct it for surface scattering. The experimental permittivity, ϵ_{exp} is now the surface scattering corrected dielectric, ϵ_C, which includes both the intra- and interband components:

$$\varepsilon_C = \varepsilon_{exp} - \frac{{\omega_p}^2}{\omega(\omega + i[\gamma_{intra} + \gamma(L_B)])} + \frac{{\omega_p}^2}{\omega(\omega + i\gamma_{intra})} \quad (2)$$

Damping due to surface scattering is calculated from

$$\gamma(L_B) = \frac{V_F}{L_B} \quad (3)$$

where V_F is the Fermi velocity, given in Table 1, and L_B is the mean free path of the electrons in the shell, calculated from[26]

$$L_B = \frac{4({r_o}^3 - {r_i}^3)}{3({r_o}^2 + {r_i}^2)} \quad (4)$$

where r_o is the outer radius and r_i is the inner radius. Moroz derives the mean free path of an electron in the billiard scattering model where reflections from the internal surfaces of the shell are specular and reports that not only does it match the experimental results for nanoshells but reduces to the well-known result for a sphere of $4r/3$.

TABLE 2: Shell Geometries for Optimized Absorption with and without Surface Scattering

	no surface scattering			with surface scattering		
element	Q_{abs}	outer radius (nm)	inner radius (nm)	Q_{abs}	outer radius (nm)	inner radius (nm)
Ag	12.2	57.4	56.5	5.7	32.8	27.2
Au	19.9	29.2	27.7	7.3	42.2	37.5
Al	13.1	5.8	0.0	10.9	6.6	0.0
Na	20.6	27.8	24.8	11.4	29.8	23.0
K	22.8	35.0	30.7	13.7	36.0	27.2

The correction method described above is limited in some circumstances. If the bulk damping is large, or for long wavelengths, the damping maybe greater than the frequency in the Drude expression (1). Additional damping then causes the surface scattering corrected imaginary permittivity to be reduced resulting in unphysically large absorption efficiency in the nanoshell. This happens in aluminum at long wavelengths and so we restrict ourselves to shells thicker than 0.8 nm in this case.

We have previously reported the optimum geometries for solid spheres of various metallic elements excluding surface scattering.[23] Most notably, gold has a maximum absorption efficiency of 3.3 for a sphere radius of 49 nm, whereas potassium reaches a maximum of 14.7 for a 21.3 nm radius sphere. Gold is far from the optimal material for spheres, at least as far as achieving maximum absorption is concerned. The inclusion of surface scattering has little effect because of the large mean free path $4/3r_o$. Even in aluminum, where the optimum size is approximately 6 nm radius, our calculation of surface scattering has little influence. The intraband damping in aluminum is so large that the additional damping due to surface scattering only causes the optimized absorption efficiency to be reduced from 13.1 to 10.9.

To optimize the geometry of the nanoshells, it is necessary to calculate the absorption efficiency as a function of aspect ratio and overall shell diameter. Here, for 350 aspect ratios between 0 and 1, we calculate the full absorption, scattering, and extinction spectrum for shells with outer radii in the range 1.0−70.0 nm. The results that give the maximum absorption efficiency for a given outer radius, inner radius, and wavelength are given in Table 2 both with and without the inclusion of surface scattering, and Figure 1 shows the associated absorption spectra.

Without including surface scattering, K has the best Q_{abs} with a value of 22.8 at a wavelength of 1144 nm, followed closely by sodium and gold and then by silver and aluminum. For the sodium and potassium shells, the increase in absorption efficiency, over that of the optimized sphere, is about 160%. With the optimum absorption efficiency for a sodium sphere occurring at a radius of 16.1 nm, with a value of 12.40. For silver, the increase between sphere and shell is just over 200% and for gold the increase is a remarkable 600%. This increase in the absorption efficiency for gold is due to the position of the band-edge at 2.25 eV which means the interband transitions are close to the resonance position for the solid sphere ($\varepsilon' = -2$) and hence decrease the absorption efficiency. For a shell, the resonance condition shifts to longer wavelengths, away from the interband transitions, as the aspect ratio decreases. Coupled with a low intraband damping, this means the absorption

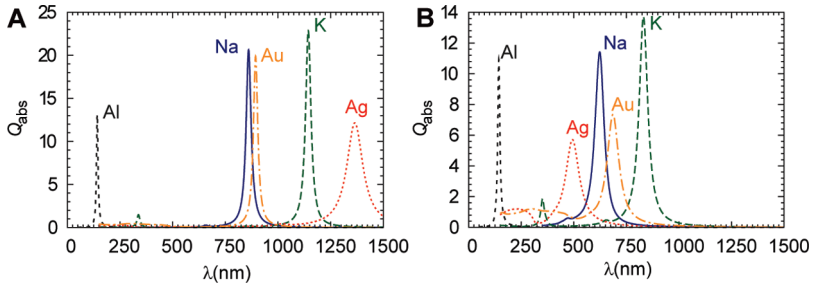

Figure 1. Optimized absorption spectra for nanoshells with radii and aspect ratios given by Table 2. (a) Without surface scattering. (b) With surface scattering.

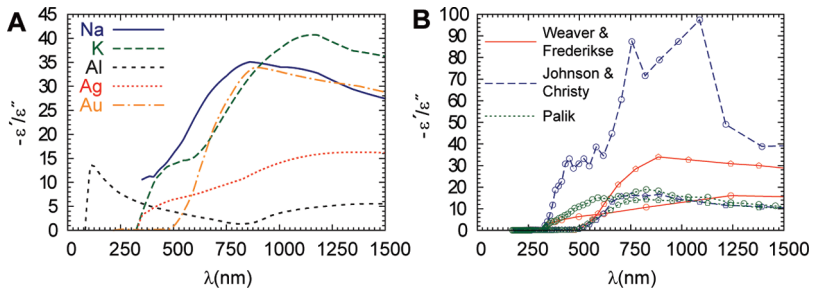

Figure 2. Quality factor $-\varepsilon'/\varepsilon''$ from experimental optical data. (a) From Weaver and Frederikse.[41] The best metal is potassium, followed by sodium, gold, silver, and aluminum. (b) The quality factor of silver (circles) and gold (pentagons) tabulated from the experiments of Weaver and Frederikse[41] (solid lines), Johnson and Christy[36] (dashed lines) and, Palik[37] (dotted lines).

efficiency can increase dramatically with increasing wavelength. For silver, the band edge is at higher frequency (3.9 eV) and does not contribute to damping for the sphere resonance, in addition, intraband damping at longer wavelengths is larger and the absorption gain from the sphere ($Q_{abs} = 5.83$ at $r = 22.9$ nm) to the nanoshell is not large. This result can be visualized by plotting the quality factor determining the strength of the resonance, $-\varepsilon'/\varepsilon''$, as a function of wavelength. This is shown in Figure 2a and is the figure of merit for nanoshells in the absence of surface scattering for the various metallic elements considered here. Na, K, and Au all perform reasonably well from about 800 nm into the infrared. This is assuming that a suitable shell can be made to access these long wavelength portions of the permittivity, whereas in reality, the shell may be so thin that surface scattering effects diminish the resonance.

There are a number of different measurements of the optical constants of the metals discussed here, and different dielectric constants may influence the outcomes of our calculations. Figure 2b compares the quality factors of silver and gold as measured by Weaver and Frederikse,[28] Johnson and Christy,[36] and Palik.[37] It is interesting to note that, although the quality factor given by Johnson and Christy's experimental dielectric constants for silver is very high between 700 and 1200 nm, most of the magnitude is derived from large negative values of ε' in this region. This results in significant damping of any resonance above about 700 nm, due to the very thin shell required. The optimum silver shell using Johnson and Christy's dielectric table has $r_i = 20.8$ nm and $r_o = 14.72$ nm with $Q_{abs} = 10.91$ at a wavelength of 413 nm. The optical constants of both Palik and Johnson and Christy have oscillations in both the real and imaginary permittivity. The data of Johnson and Christy shows a peak after the well-known band edge in silver at 3.9 eV, and although a Drude tail can be drawn through the error bars in the data, large scale oscillations cause an unusual shifting in both peak positions and magnitudes compared to the other data.

For wavelengths above 1200 nm, the optical constants of Palik are each comprised of two different data sets, in Figure 2b, we present only the data of Winsemius et al.[38] for silver and Théye[39] for gold, and neglect the data of Dold and Mecke,[40] which is only available above 1200 nm and disagrees with the other data compiled by Palik.

The data of Weaver and Frederikse and Palik give similar results and would lead to the same conclusions in the current work. Optimized absorption efficiencies of shells with outer radii in the region 1.0−70.0 nm remain similar, although the optimum shell thickness varies due to differences in the real part of the permittivity. By contrast, the data of Johnson and Christy, discussed above, are different, and they have only published for silver and gold. In order to obtain a consistent set of data, where we can compare between the various elements, we choose dielectric constants compiled by one set of authors.

The optimum geometry for an aluminum nanoshell is just the sphere (Table 2 and Figure 1), due to the relationship between the real and imaginary parts of the permittivity. In the limit of no interband transitions, and for frequencies below the plasma frequency, we can approximate the $-\varepsilon'/\varepsilon''$ relationship with ω/γ, indicating that for a Drude-like metal, the best resonance will occur at the highest possible frequency. For aluminum, the best $-\varepsilon'/\varepsilon''$ ratio occurs at 112 nm, which is below the threshold wavelength for the excitation of a resonance (as $\varepsilon' = -0.93$).

From the above discussion, it is clear that surface scattering corrections need to be applied in order to understand the response of nanoshells at longer wavelengths where the shell can be quite thin. Figure 3 shows the results of optimization calculations with the bulk dielectric corrected for surface scattering. In each case an outer radius is chosen, and then the optimum aspect ratio is determined for that outer radius.

The intial peak in the data of Figure 3a for Na, K, Al, and Ag represents the maximum absorption efficiency for a sphere. A cusp is apparent in the data of Na, K, and Ag where the optimum geometry moves from being a solid sphere with aspect ratio 1 to being a shell. This point in Figure 3a appears as a vertical line in Figure 3b. The vertical lines in Figure 3c also reflects the point at which a solid sphere gives the optimum absorption efficiency and correspond to the point at which the

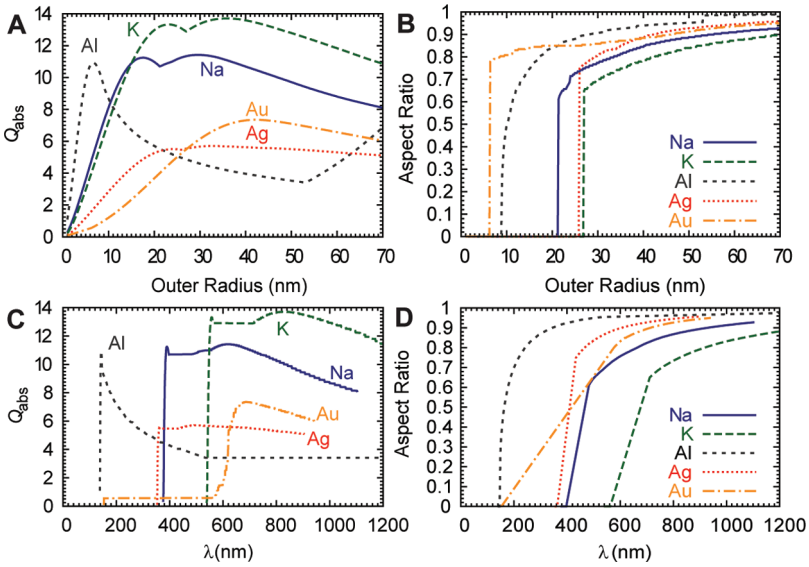

Figure 3. Optimized absorption efficiency for nanoshells including surface scattering. (a) Maximum absorption efficiency: for each radius an optimum wavelength and aspect ratio is determined. (b) The aspect ratio that gives the maximum absorption efficiency in panel a. (c) Maximum absorption efficiency as a function of wavelength: vertical lines correspond to sphere resonances, and they appear as vertical lines in panel b, and are visible in panel a before the first peak. (d) Aspect ratio responsible for maximum absorption efficiency in panel c.

aspect ratio becomes zero in Figure 3d. The plot of absorption versus wavelength is very steep at this point because the plasmon resonance of a sphere does not shift very much with sphere size. Upon close inspection, a very slight curve can be seen for sodium and potassium, as a low plasma frequency causes more variation in peak position with wavelength. Au is different because for quite small outer radii, less than about 10 nm, single electron interband transitions dominate the absorption. This is why the absorption in Au extends down to wavelengths shorter than 200 nm when the plasmon resonance of the sphere is only about 530 nm.

The inclusion of surface scattering has reduced the optimum absorption efficiency of sodium and potassium nanoshells by 45% and 40%, respectively, which is a large improvement over the reduction in silver and gold which stand at 53% and 63%, respectively. From Figure 3c Na provides the best absorption over the shorter wavelength visible region and K over the red to near-infrared region. The aspects ratios of the corresponding shells are also reasonable within these regimes for these two elements (Figure 3d) with Na being less than about 0.7 and K less than 0.9. By contrast the aspect ratios in gold or silver required to access these regions are greater than 0.9. This is the reason why these two elements do not perform well; they are limited by surface scattering.

The absorption efficiency of aluminum nanoshells has shifted extensively into the infrared in the large radius limit upon the inclusion of surface scattering. This appears counterintuitive as not only have we restricted the shell thickness to 0.8 nm but also because the other metal nanoshell resonances are blue-shifted when surface scattering is included. However, the red-shift is a general function of the low energy interband transition that disrupts the ε'' spectrum of aluminum. The overall effect of the transition runs from 400 to 1100 nm, which causes the resonance to make a jump across a range of wavelengths. This jump requires a dramatic reduction in the shell thickness, furthermore, the resonance enters the long wavelength regime and the previously discussed anomalous absorption effect starts to appear, driving an increase in the absorption efficiency for shells with $r_o > 53.0$ nm (see Figure 3 a,b)

We have used Mie theory and the billiard scattering model to calculate the optimized absorption efficiencies of nanospheres and vacuum core−metal shell nanoparticles made of aluminum, sodium, potassium, silver, and gold.

The effect of the introduction of surface scattering (using the billiard scattering model) on optimized solid nanospheres has shown to be small, with aluminum spheres suffering a 17% reduction in absorption efficiency, and the other metals suffering less than 10% reduction in Q_{abs}, with minor red shifting of the position of the resonance to allow for larger spheres. Potassium metal spheres had the highest absorption efficiency, over 400% larger than that of the optimized gold nanosphere.

The effect of surface scattering is more profound on nanoshells, with all of the optimized resonances blue-shifting to compensate for a general increase in shell thickness. This effect resulted in a bias toward low plasma frequency metals as $-\partial\varepsilon'/\partial\lambda$ is close to zero, resulting in a tunability across the spectrum that enables the resonance to be placed in the (usually high wavelength) $-\varepsilon'/\varepsilon''$ maximum, without a huge decrease in the shell thickness. We showed that for a Drude metal, the optimum geometry is a sphere as $-\varepsilon'/\varepsilon'' \approx \gamma/\omega$; however, interband transitions usually disrupt this. The introduction of surface scattering for aluminum nanoshells was troublesome, as additional damping from surface scattering resulted in a negative correction to the imaginary part of the permittivity, resulting in anomalously high absorption efficiency. Silver and gold nanospheres suffered a reduction in absorption efficiency due to high plasma frequencies that caused the resonances to blue-shift away from the $-\varepsilon'/\varepsilon''$ maximum.

Sodium and potassium nanoshells offer a considerable maximum absorption efficiency advantage over both silver and gold nanoshells, offering up to an 86% increase over the Q_{abs} of gold nanoshells and a 240% increase over silver. This dramatic increase may be worth the additional inconveniencies of handling these reactive metals.

Acknowledgment. This work was supported by the Australian Research Council and the University of Technology, Sydney. Computing resources were provided by the Australian Centre for Advanced Computing and Communication (ac3) in New South Wales and the National Facility at the Australian Partnership for Advanced Computing (APAC).

References and Notes

(1) Melville, D. O. S.; Blaikie, R. J. *Opt. Express* **2005**, *13* (6), 2127–2134.

(2) Fang, N.; Lee, H.; Sun, C.; Zhang, X. *Science* **2005**, *308* (5721), 534–537.

(3) Blaber, M. G.; Arnold, M. D.; Harris, N.; Ford, M. J.; Cortie, M. B. *Physica B* **2007**, *394* (2), 184–187.

(4) Hirsch, L. R.; Stafford, R. J.; Bankson, J. A.; Sershen, S. R.; Rivera, B.; Price, R. E.; Hazle, J. D.; Halas, N. J.; West, J. L. *Proc. Natl. Acad. Sci* **2003**, *100*, 13549.

(5) Pissuwan, D.; Valenzuela, S. M.; Cortie, M. B. *Trends Biotechnol.* **2006**, *24* (2), 62–67.

(6) Pissuwan, D.; Valenzuela, S. M.; Killingsworth, M. C.; Xu, X. D.; Cortie, M. B. *J. Nanopart. Res.* **2007**, *9* (6), 1109–1124.

(7) Pissuwan, D.; Valenzuela, S. M.; Miller, C. M.; Cortie, M. B. *Nano Lett.* **2007**, *7* (12), 3808–3812.

(8) Kawata, S.; Ono, A.; Verma, P. *Nat. Photonics* **2008**, advanced online publication.

(9) Engheta, N. *Science* **2007**, *317* (5845), 1698–1702.

(10) Kim, S.; Jin, J.; Kim, Y.-J.; Park, I.-Y.; Kim, Y.; Kim, S.-W. *Nature* **2008**, *453* (7196), 757–760.

(11) Cortie, M.; Xu, X.; Chowdhury, H.; Zareie, H.; Smith, G. *Proc. SPIE* **2005**, *5649*, 565.

(12) Pena, O.; Pal, U.; Rodriguez-Fernandez, L.; Crespo-Sosa, A. *J. Opt. Soc. Am. B: Opt. Phys.* **2008**, *25* (8), 1371–1379.

(13) Harris, N.; Ford, M. J.; Cortie, M. B. *J. Phys. Chem. B* **2006**, *110* (22), 10701–10707.

(14) Harris, N.; Ford, M. J.; Mulvaney, P.; Cortie, M. B. *Gold Bull.* **2008**.

(15) Jain, P. K.; Lee, K. S.; El-Sayed, I. H.; El-Sayed, M. A. *J. Phys. Chem. B* **2006**, *110* (14), 7238–7248.

(16) Nikoobakht, B.; El-Sayed, M. A. *Chem. Mater.* **2003**, *15*, 1957–1962.

(17) Sun, Y. G.; Mayers, B. T.; Xia, Y. N. *Nano Lett.* **2002**, *2* (5), 481–485.

(18) Liu, J. Q.; Cankurtaran, B.; Wieczorek, L.; Ford, M. J.; Cortie, M. *Adv. Funct. Mater.* **2006**, *16* (11), 1457–1461.

(19) Cortie, M. B.; Dowd, A.; Harris, N.; Ford, M. J. *J. Phys. Rev. B: Condens. Matter* **2007**, *75* (11), 113405.

(20) van der Zande, B. M. I.; Böhmer, M. R.; Fokkink, L. G. J.; Schönenberger, C. *Langmuir* **2000**, *16*, 451–458.

(21) Gentle, A.; Maaroof, A.; Smith, G.; Cortie, M. *Proc. SPIE* **2006**, *6038*, 603816.

(22) Loo, C.; Lowery, A.; Halas, N.; West, J.; Drezek, R. *Nano Lett.* **2005**, *5* (4), 709–711.

(23) Blaber, M.; Harris, N.; Ford, M. J.; Cortie, M. B. Nanoscience and Nanotechnology 2006. ICONN ′06. International Conference on. *Proc. IEEE* **2006**, 561.

(24) Berciaud, S.; Cognet, L.; Tamarat, P.; Lounis, B. *Nano Lett.* **2005**, *5* (3), 515–518.

(25) Schelm, S.; Smith, G. B. *J. Opt. Soc. Am. A* **2005**, *22* (7), 1288–1292.

(26) Moroz, A. *J. Phys. Chem. C* **2008**, *112* (29), 10641–10652.

(27) Bohren, C. F.; Huffman, D. R. *Absorption and scattering of light by small particles*; Wiley: Weinheim, Germany, 2004.

(28) Weaver, J. H. Frederikse, H. P. R. *Optical properties of selected elements*, 82nd ed.; CRC Press: Boca Raton, FL, 2001.

(29) Kreibig, U.; Fragstein, C. v. *Z. Phys. A* **1969**, *224* (4), 307–323.

(30) Ashcroft, M. *Solid State Physics*, College ed.; Saunders College Publishing: Philadelphia, PA, 1976.

(31) Noguez, C.; Román-Velázquez, C. E. *Phys. Rev. B Condens. Matt.* **2004**, *70* (19), 195412.

(32) Link, S.; El-Sayed, M. A. *Int. Rev. Phys. Chem.* **2000**, *19* (3), 409–453.

(33) Kittel, C. *Introduction to Solid State Physics*, 7th ed.; John Wiley and Sons: New York, 1996.

(34) LaVilla, R.; Mendlowitz, H. *Phys. Rev. Lett.* **1962**, *9* (4), 149.

(35) Smith, N. V.; Spicer, W. E. *Phys. Rev.* **1969**, *188* (2), 593.

(36) Johnson, P. B.; Christy, R. W. *Phys. Rev. B* **1972**, *6* (12), 4370.

(37) Palik, E. D. *Handbook of Optical Constants of Solids*; Academic Press: New York, 1985.

(38) Winsemius, P.; Kampen, F. F. v.; Lengkeek, H. P.; Went, C. G. v. *J. Phys. F* **1976**, *6* (8), 1583–1606.

(39) Thèye, M.-L. *Phys. Rev. B* **1970**, *2* (8), 3060.

(40) Dold, B.; Mecke, R. *Optik* **1965**, *22*, 435.

(41) Weaver, J. H.; Olson, C. G.; Lynch, D. W. *Phys. Rev. B* **1975**, *12* (4), 1293.

JP810808H